

# Dynamic mechanical analysis of nylon 6 fiber-reinforced acrylonitrile butadiene rubber composites

Polymers and Polymer Composites  
2021, Vol. 29(9S) S1328–S1339  
© The Author(s) 2021  
Article reuse guidelines:  
[sagepub.com/journals-permissions](https://sagepub.com/journals-permissions)  
DOI: 10.1177/096739112111046144  
[journals.sagepub.com/home/ppc](https://journals.sagepub.com/home/ppc)



C Rajesh<sup>1</sup> , P Divia<sup>1</sup>, S Dinooplal<sup>2</sup>, G Unnikrishnan<sup>3</sup> and E Purushothaman<sup>4</sup>

## Abstract

Dynamic mechanical properties of polymeric materials are of direct relevance to a range of unique polymer applications. The aim of the study is to investigate the dynamic mechanical properties of composites of short nylon 6 fiber with acrylonitrile butadiene rubber (NBR). The storage modulus ( $G'$ ), loss modulus ( $G''$ ), and the damping factor ( $\tan \delta$ ) have been analyzed with reference to the effects of fiber loading, curing systems, and bonding agents over a range of temperature and at varying frequencies. The storage modulus increases with increment in fiber loading, whereas loss modulus and damping factor decrease. The glass transition temperature shifts to higher temperature upon increment in fiber loading. Dicumyl peroxide (DCP)-cured composites show higher storage modulus and lower damping than the corresponding sulfur-cured one. The addition of hexa-resorcinol and phthalic anhydride as bonding agents enhances the dynamic mechanical properties of the composites. The experimental results have been evaluated by comparing with Einstein, Guth, and Nielsen models.

## Keywords

Nylon 6, acrylonitrile butadiene rubber, composites, dynamical mechanical analysis, storage modulus, loss modulus, damping

Received 26 November 2020; accepted 26 August 2021

## Introduction

Rubbers show both elastic and damping behavior because of their visco-elastic nature. When they are deformed by a sinusoidal stress, the resulting strain will also be sinusoidal but will be out of phase with the applied stress. Dynamic losses are usually associated with specific mechanisms of molecular or structural motion in polymeric materials. The damping in the system can be measured from the tangent of the phase angle or loss tangent ( $\tan \delta$ ) which is defined as  $\tan \delta = G''/G'$  where  $G'$  is the storage modulus due to stored elastic energy in the materials and  $G''$  is the loss modulus due to viscous dissipation. The method that has been used to investigate the storage modulus, loss modulus, and loss tangent is dynamical mechanical analysis (DMA).

In DMA, the response of a given material to an oscillatory deformation is measured as a function of temperature. This technique has widely been employed for investigating the visco-elastic behavior, stiffness (modulus), damping (energy dissipation) characteristics, phase transitions, and the interfacial adhesion of polymer composites as they are deformed under periodic stresses.<sup>1–2</sup> It is particularly useful because of its non-destructive nature unlike other static mechanical testing methods.

Polymers at the transition region from glassy to rubbery state have great potential for vibration damping. The intensity and breadth of the damping factor ( $\tan \delta$ ) peak and the value of the loss modulus generally determine the damping capacity of a polymer at that particular temperature. For fiber-reinforced polymer composites, the dynamic mechanical properties depend on the type of fiber, length of the fiber, orientation of fiber, fiber loading (phr), fiber dispersion in matrix, and interaction between fiber and matrix.<sup>3–4</sup>

Several researchers have studied the dynamic mechanical properties of rubber composites. Malas et al. studied the reinforcing effect of expanded graphite (EG) and modified EG (MEG) with and without carbon black (CB) on the properties of emulsion polymerized styrene butadiene rubber (SBR) vulcanizates.<sup>5</sup> Flaifel et al. carried out the thermal conductivity and

<sup>1</sup>Department of Chemistry, MES Keveeyam College Valanchery, Kerala, India

<sup>2</sup>Department of Chemistry, St Thomas College, Trissur, Kerala, India

<sup>3</sup>Department of Chemistry, National Institute of Technology, Calicut, Kerala, India

<sup>4</sup>Department of Chemistry, University of Calicut, Kerala, India

## Corresponding author:

C Rajesh, Department of Chemistry, MES Keveeyam College Valanchery, Malappuram Dt., Valanchery, Kerala 676552, India.

Email: [rajeshvly@rediffmail.com](mailto:rajeshvly@rediffmail.com)

dynamic mechanical analysis of Ni–Zn ferric nanoparticle-filled thermoplastic natural rubber nanocomposites.<sup>6</sup> Dynamic mechanical analysis of polylactic acid (PLA)-hemp bio-composites with different reinforcement content was carried out by Durante et al.<sup>7</sup> Recently, Surajarusam et al. conducted a comparative study of pineapple leaf microfiber and aramid fiber-reinforced natural rubbers using dynamic mechanical analysis.<sup>8</sup> The dynamic properties like damping factor, storage, and loss moduli of areca/kenaf fiber-reinforced epoxy hybrid composites were studied by Palani et al.<sup>9</sup> Dynamic mechanical analysis of natural nano banana particle-filled polymer matrix composites was conducted by Surya et al., and it was found that incorporation of nano banana particles in polyester matrix induces reinforcing effects appreciably at higher temperatures.<sup>10</sup> Recycled tire rubber was utilized as a filler to fabricate wood-high density polyethylene (HDPE) composite by Feiyu et al., and it was found that rubber-filled materials exhibit advantageous energy absorption performance compared to wood-HDPE composites under repetitive compressions.<sup>11</sup>

Acrylonitrile butadiene rubber (NBR) is a synthetic elastomer widely used in many industrial applications especially in automotive products. It has good resistance to fuel and oil even at elevated temperatures. On the industrial side, NBR finds uses in roll covers, hydraulic hoses, conveyor belting, graphic arts, oil field packers, and seals for all kinds of plumbing and appliance applications. In the automotive area, NBR is used in fuel and oil handling hoses, seals, and grommets. Nylon 6 fiber is a semicrystalline polyamide. It has high melting point, tensile strength, and modulus. The objective of the present work is to examine the dynamic mechanical properties of nylon 6 fiber-reinforced NBR composites at varying frequencies and temperatures with special reference to the effects of fiber loading, curing systems, and bonding agents.

## Experiment

### Materials

Acrylonitrile butadiene rubber (Apar Industries, Mumbai, India) having 35% acrylonitrile content and nylon 6 fiber (Sri Ram Fibers Polymers Limited, Chennai, India) in yarn form were used in the study. The rubber ingredients such as vulcanizing agents, accelerators, and activators used were of commercial grade. Hexamethylene tetramine, resorcinol, and phthalic anhydride used as bonding agents were of laboratory reagent grade.

### Composite Preparation

Table 1 shows the formulations of the mixes used in the present work. The composites were prepared using a laboratory two roll rubber mixing mill (150 × 300 mm). NBR was masticated on the mill for 2 min, and then, the compounding ingredients were added. In all the mixes, the nip gap, mill roll speed ratio, and the number of passes were kept constant. The samples were milled for sufficient time to ensure the dispersion of fibers. Vulcanization of the mixes was done at 153°C in a hydraulic press having electrically heated platens to their respective cure times as obtained from a Monsanto Rheometer.

### Dynamic mechanical analysis (DMA)

Dynamic mechanical thermal analyzer (NETZSCH DMA 242) was used to measure the dynamic storage modulus ( $G'$ ), loss modulus ( $G''$ ), mechanical damping ( $\tan \delta$ ), and the glass transition temperature ( $T_g$ ). The temperature range through which

**Table 1.** Formulations of mixes (phr<sup>a</sup>).

	A	B	C	D	E	F	G
NBR <sup>b</sup>	100	100	100	100	100	100	100
Zinc oxide							5
Stearic acid							2
MBTS <sup>c</sup>							1.5
TMTD <sup>d</sup>							0.5
Sulfur							1.5
DCP <sup>e</sup>	5	5	5	5	5	5	
Hexa <sup>f</sup>					1.92		
Resorcinol					3.84		
Phthalic anhydride						3	
Nylon fiber		126	18	24	24	24	24
Fiber length (mm)			6	6	6	6	6

<sup>a</sup>Parts per hundred rubber.

<sup>b</sup>Acrylonitrile butadiene rubber.

<sup>c</sup>Mercapto benzo thiazyl disulphide.

<sup>d</sup>Tetramethyl thiuram disulphide.

<sup>e</sup>Dicumyl peroxide.

<sup>f</sup>Hexamethylene tetramine.

the properties were determined was  $-110$  to  $104^{\circ}\text{C}$ , at a heating rate of  $2^{\circ}\text{C}/\text{minute}$ . Three-point bending method was used as forced vibration at varying frequencies such as 0.1, 1, 10, and 50 Hz with strain amplitude of  $120\ \mu\text{m}$ .

## Results and discussion

### Effect of fiber loading

The variation of storage modulus ( $G'$ ) with fiber loading of nylon 6/NBR composites as a function of temperature, at a frequency of 10 Hz is given in Figure 1. The gum compound, without fibers, has the lowest stiffness and hence the lowest storage modulus at a given temperature. The fibers can participate in effective stress transfer, and as a result, the stiffness of the composites increases leading to higher storage modulus. The hydrodynamic effects of the fibers embedded in a visco-elastic medium and the mechanical restraint introduced by them at their higher concentrations reduce the mobility and the deformability of the matrix.<sup>12</sup>

It has been observed that the storage modulus increases with increasing fiber loading at all temperatures. As the fiber loading is increased, the stress is more evenly distributed and the storage modulus of the composite increases. Similar observation is reported by other authors for fiber-reinforced rubber composites.<sup>13</sup> The increment in  $G'$  is prominent in the glassy state, below  $T_g$ , while it is not so significant in the rubbery plateau region. It can be seen that in the glassy region, the modulus values gradually increase while in the rubbery region, the change is relatively very less. In the glassy region, the components are in a frozen state, that is, highly immobile. In such a state, there exists a close and tight packing in the composite structure resulting in higher modulus. It is important to mention that the modulus in the glassy state is determined primarily by the strength of the intermolecular forces and the way the polymer chains are packed. As temperature increases, the components become more mobile and lose their close packing arrangement. As a result, in the rubbery region, there is no significant change in the modulus.

The effectiveness of fillers on the moduli of composites can be represented by a coefficient  $C$  which is given as<sup>14</sup>

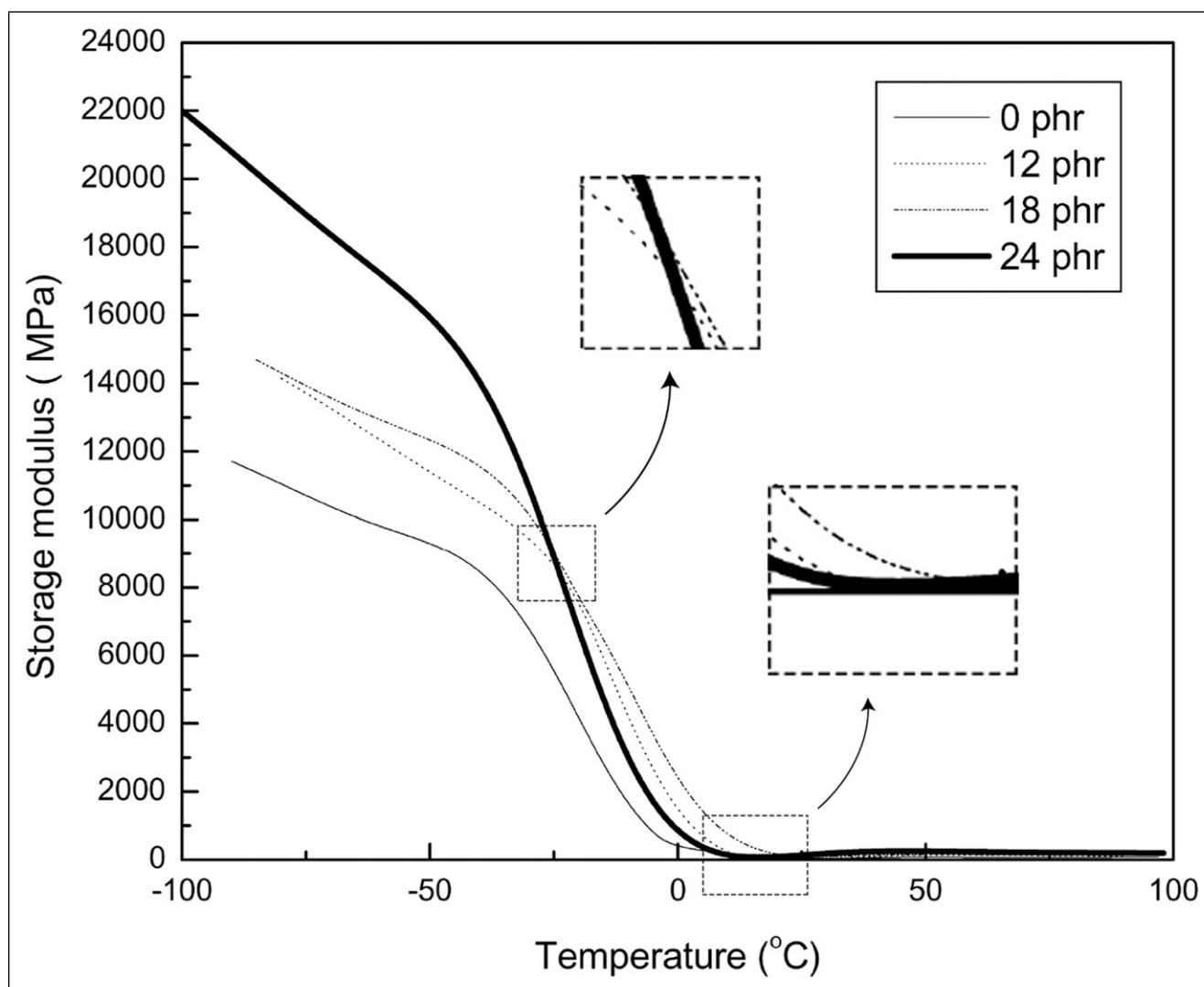


Figure 1. Effect of fiber loading on storage modulus as a function of temperature at a frequency of 10 Hz.

$$C = \frac{G'_g / G'_{r,comp}}{G'_g / G'_{r,resin}} \quad (1)$$

where  $G'_g$  and  $G'_r$  are the storage modulus values in the glassy and rubbery region, respectively. The lower the value of the constant  $C$ , the better is the effectiveness of the filler. The values obtained for different systems at a frequency of 10 Hz are given in Table 2. The value of  $C$  decreases with fiber loading up to 24 phr which shows the increased reinforcing effect of fibers. From Figure 1, it can also be seen that the storage modulus of all systems decreases with increase in temperature. The relaxation of macromolecular chains occurs at higher temperature, which disturbs the close packing of fibers resulting in the deterioration of the composite structures thus lowering the storage modulus.<sup>15</sup>

Figure 2 shows the variation of loss modulus ( $G''$ ) with temperature as a function of fiber loading at a frequency of 10 Hz. Loss modulus measures the energy dissipated or lost as heat per cycle of sinusoidal deformation. It is in fact the viscous response of the material. Loss factors are more sensitive to molecular motions. The loss modulus values generally increase with increase in fiber concentration at temperatures well below the glass transition. The loss modulus peak values are less for composites than for the gum in the region of transition. A specific interaction between the filler and the polymer layer would create a layer of immobilized polymer between the filler and matrix. The matrix surrounding the fibers can be taken as an inter-layer which is in a different state compared to the rest of the matrix where the molecular motions are relatively hindered.<sup>16</sup> A shell of immobilized polymer surrounds the fibers,<sup>17</sup> and the higher the volume fraction of the matrix, the more the restraint at the interface.

The effect of fiber loading on the damping factor ( $\tan \delta$ ) as a function of temperature at a frequency of 10 Hz is illustrated in Figure 3. The  $\tan \delta$  values can be related to the impact resistance of the material as it expresses the out-of-phase time relationship between an impact force and the resultant force that is transmitted to the supporting body. The damping in composites is due to the shear stress concentration at the fiber ends and visco-elastic energy dissipation in the matrix material. It can be seen from Figure 3 that  $\tan \delta$  value is highest for the gum sample and it decreases with increase in fiber loading. The decrease in  $\tan \delta$  values is due to the improvement in the interfacial bonding in composites with increment in fiber loading. When the fiber concentration is less, the packing of fibers will not be efficient in the composites. This leads to matrix rich regions and thus to an easier failure of the bonding at the interfacial region. At higher fiber loading, when there is relatively high close packing of fibers, crack propagation will be prevented by the neighboring fibers.

The fibers restrict the movement of polymeric chains, causing the reduction in the peak of the  $\tan \delta$ . The temperature at which maximum damping occurs ( $\tan \delta_{max}$ ) represents the glass transition temperature ( $T_g$ ) of the system. As the fiber loading increases, the  $\tan \delta_{max}$  decreases and the  $T_g$  values show a positive shift (Table 2). The shifting of  $T_g$  to higher temperatures can be associated with the decreased mobility of the chains by the addition of fibers. Elevation in  $T_g$  is taken as a measure of interfacial interaction.

**Table 2.** Effect of Fiber Loading on the Characteristics of Composites at a Frequency of 10 Hz.

Fiber loading (phr)	Value of coefficient, C	$\tan \delta$ (max)	$T_g$ ( $^{\circ}$ C)	Energy of activation for glass transition ( $E_a$ ) (kJ/mol)
0	1.0	0.67	-9.0	174.06
12	0.97	0.50	-0.5	212.75
18	0.22	0.41	1.4	223.38
24	0.12	0.40	1.9	239.34

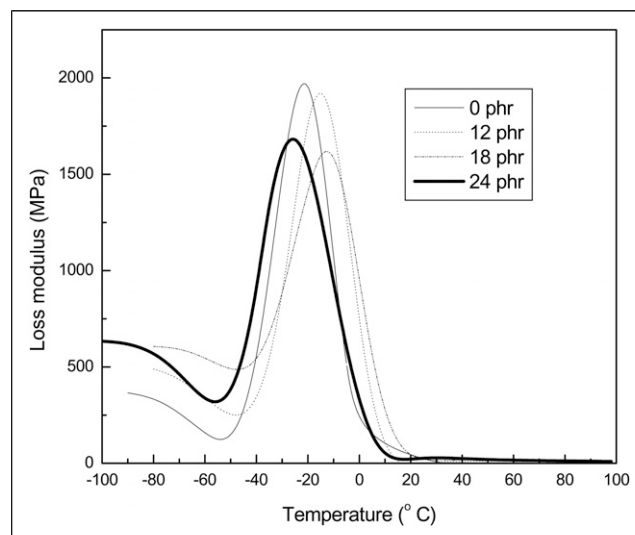


**Figure 2.** Effect of fiber loading on loss modulus as a function of temperature at a frequency of 10 Hz.

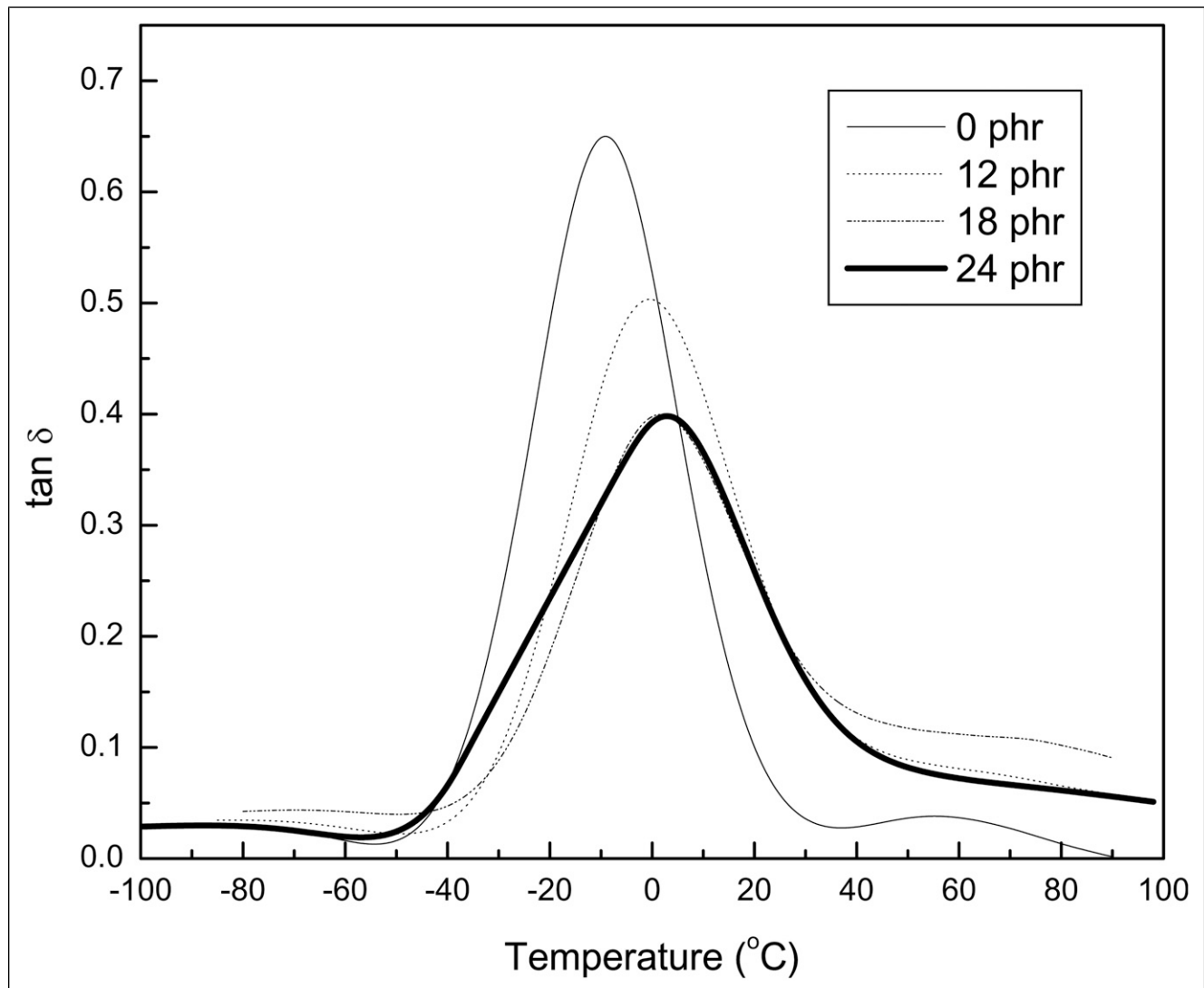


**Figure 3.** Effect of fiber loading on damping characteristics ( $\tan \delta$ ) as a function of temperature at a frequency of 10 Hz.

### Effect of curing agents

Effect of different curing systems on the dynamic mechanical properties of composites was studied with reference to samples containing optimum loading of fiber. Optimization of fiber loading has already been done by our group by studying the static mechanical properties of composites.<sup>18</sup> It can be seen from [Figure 4](#) that at optimum fiber loading (24 phr), the storage modulus of DCP cured sample is higher than that of sulfur cured one. The difference in this behavior can be attributed to the difference in cross-links introduced by DCP and sulfur. DCP introduces rigid C–C linkages, whereas sulfur creates mono, di, and polysulfidic linkages during curing. These results are in well agreement with the observations from the static mechanical tests of the present composite system and the measurement of cross-link density through restricted equilibrium technique.<sup>18-19</sup> The variation of  $\tan \delta$  with temperature of DCP- and sulfur-cured samples is given in [Figure 5](#). It can be seen that DCP-cured sample shows lower  $\tan \delta_{\max}$  compared to corresponding sulfur-cured one.

### Effect of bonding agents

[Figure 6](#) shows the effect of two bonding agents, viz., hexa-resorcinol and phthalic anhydride on the storage modulus ( $G'$ ), as a function of temperature, at a frequency of 10 Hz. It is evident that the  $G'$  values of composites containing bonding agents are higher than that of the unbonded one at 24 phr fiber loading. This is due to the better interfacial adhesion in bonding agent-added composites. The variation of  $\tan \delta$  with temperature for composites with and without bonding agent at the frequency of 10 Hz is given in [Figure 7](#). It is obvious that the presence of bonding agent reduces the  $\tan \delta$  values. Bonding agent-added composites show lower value of  $\tan \delta_{\max}$  than that of the unbonded one. Also, the  $T_g$  values are shifted to higher temperatures due to greater interfacial interaction. The broadening of  $\tan \delta$  peak is also indicative of the improved interfacial adhesion in bonding agent-added composites.

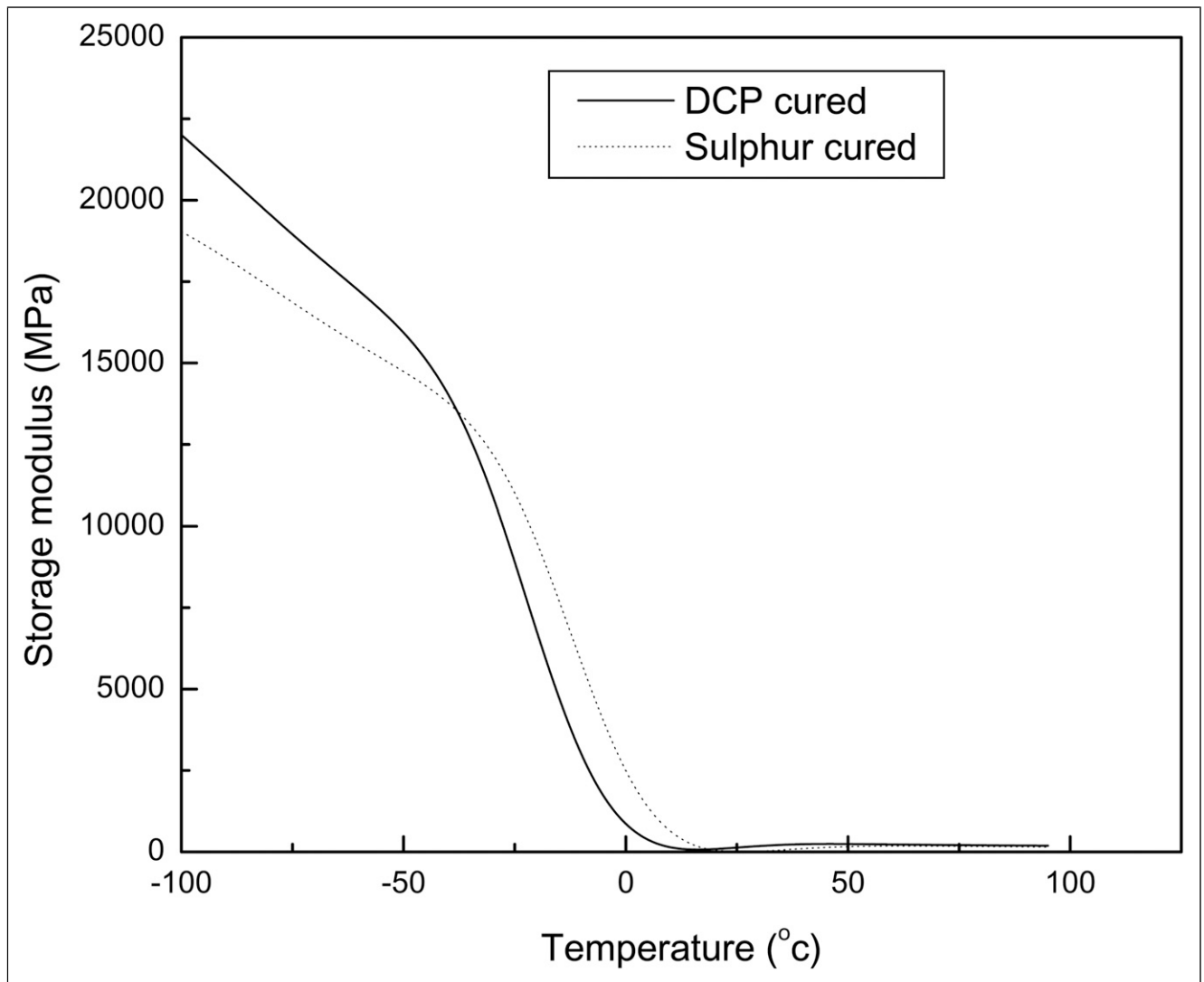


**Figure 4.** Variation of storage modulus of dicumyl peroxide- and sulfur-cured samples with temperature at a frequency of 10 Hz.

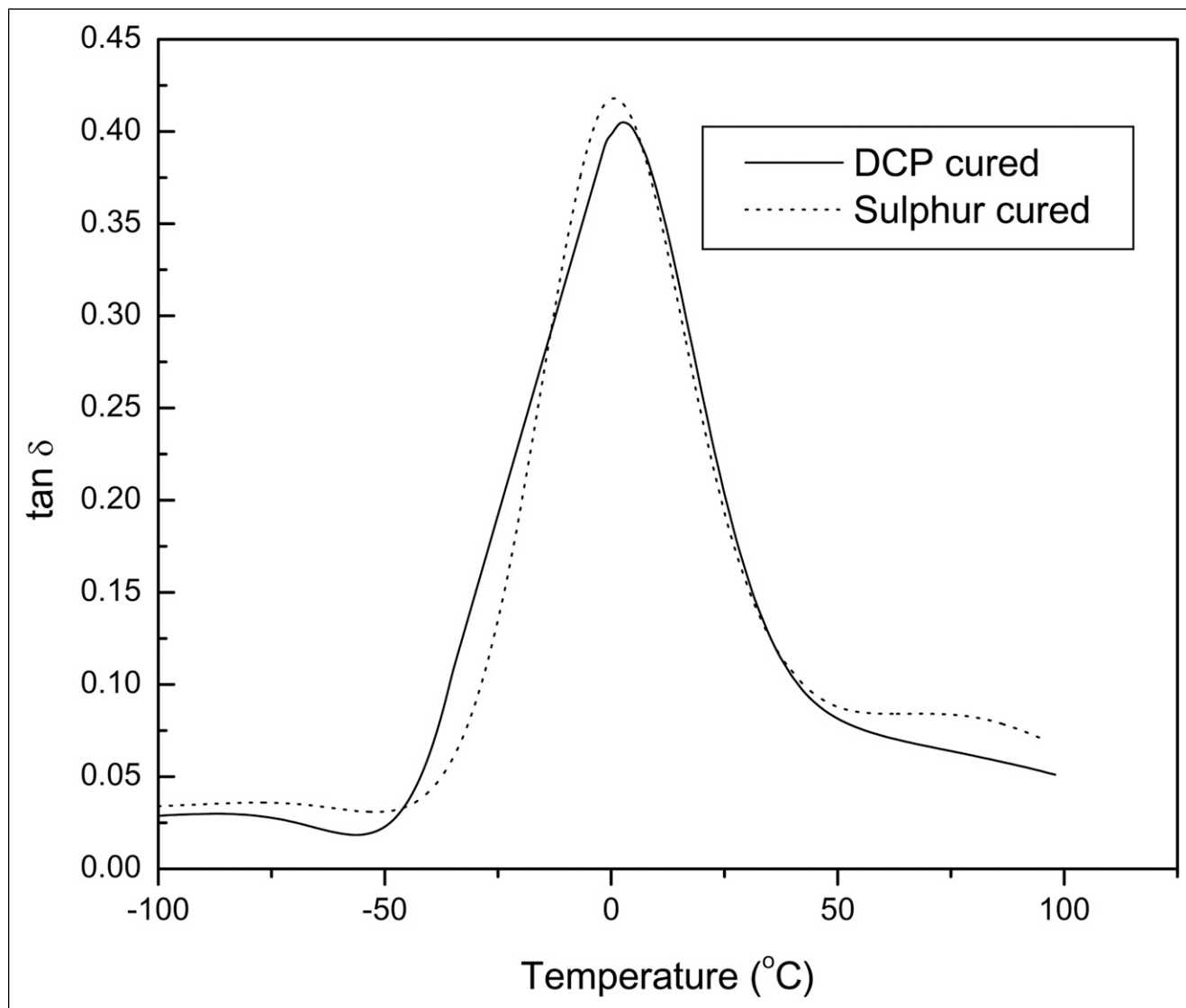
### Effect of frequency

Figure 8 shows the variation of storage modulus ( $G'$ ) of composite sample containing 24 phr fibers (Mix D) as a function of temperature at different frequencies. It can be seen that the storage modulus increases with frequency from 0.1 to 50 Hz. At high frequency (short time), the modulus measurements results in higher values, whereas low frequency (long time) result in lower values.<sup>2</sup> The lesser mobility of polymeric chain at higher frequencies results in better bonding between the fibers and matrix, which thereby increases the stiffness of the composite.

Figure 9 shows the effect of frequency on damping factor ( $\tan \delta$ ) of composite sample containing 24 phr fibers (Mix D, Table 1) as a function of temperature. At lower temperature regions, the  $\tan \delta$  values are found to be decreased with an increase in frequency. However, the reverse occurs in the higher temperature regions. Below  $T_g$ , the deformation by the fillers is non-virtual, the components are in a frozen state, that is, highly immobile, and hence, the damping is mainly dependent on the segmental mobility of the matrix. In such a case, an increment in frequency can induce the segmental mobility or molecular motions of the matrix resulting in lower damping properties. However, in higher temperature regions (above  $T_g$ ), as the frequency increases, the molecules will not get time to undergo rearrangement, and as a result, the material behavior will be more like a liquid with enhanced damping properties. Due to the same reason, it has been observed that the temperature corresponding to  $\tan \delta_{\max}$  or  $T_g$  is shifted to the high temperature region at higher frequencies.

### Energy of activation for glass transition

The apparent activation energy ( $E_a$ ), for the glass transition of different composite systems, was calculated using the modified form of Arrhenius relationship<sup>20</sup>



**Figure 5.** Variation of  $\tan \delta$  of dicumyl peroxide- and sulfur-cured samples with temperature at a frequency of 10 Hz.

$$\log^{\circ}V = \log^{\circ}v_0 - \left( \frac{E_a}{2.303 R T_{\max}} \right) \quad (2)$$

where  $v$  is the measuring frequency;  $v_0$  is the frequency when temperature  $T$  approaches infinity;  $R$ , the gas constant;  $T_{\max}$ , the temperature corresponding to the maximum of  $\tan \delta$  curve; and  $E_a$ , the energy of activation for glass transition, obtained from the slope of the typical Arrhenius plot of  $\log v$  against  $1/T$ . Energy of activation ( $E_a$ ) for the glass transition, for nylon 6 fiber-reinforced NBR composites as a function of fiber loading is given in Table 2. As fiber loading increases, the process of transition becomes more difficult to occur and takes place at higher temperatures by consuming larger quantity of energy which is indicated by a shift in  $T_g$  to higher temperatures. At lower levels of loading, the fiber/matrix interaction will be less, and hence, the activation energy is also low. The systems with higher activation energy have lower chain mobility and a better interfacial adhesion. Thus, the calculations of activation energy can be used as a criterion for measuring the interfacial adhesion between the fibers and the matrix.

### Cole–Cole plots

Figure 10 shows the Cole–Cole plots of various composite systems, where the loss modulus data ( $\log G''$ ) are plotted as a function of the storage modulus ( $\log G'$ ) at a frequency of 10 Hz. The nature of Cole–Cole plot is indicative of the nature of the system. Homogeneous polymeric systems show a semicircle diagram,<sup>2</sup> whereas the two-phase systems show modified semicircles.<sup>21</sup> On analyzing the Cole–Cole plots of the present composite systems, it is seen that the curves show the shape of imperfect semicircles. The shape of the curves thus points toward good fiber-rubber adhesion.

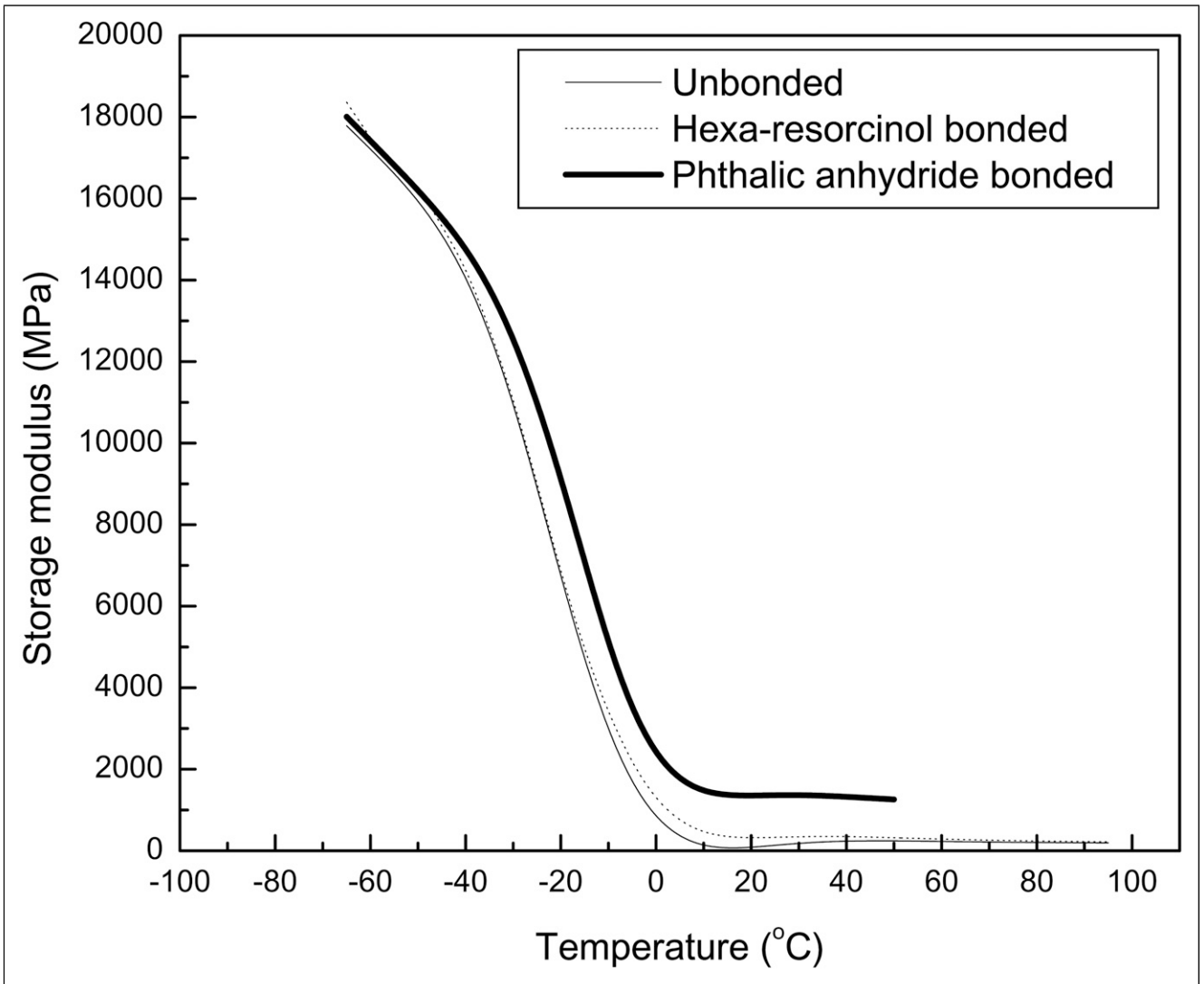


Figure 6. Variation of storage modulus with temperature of unbonded and bonded composites at a frequency of 10 Hz.

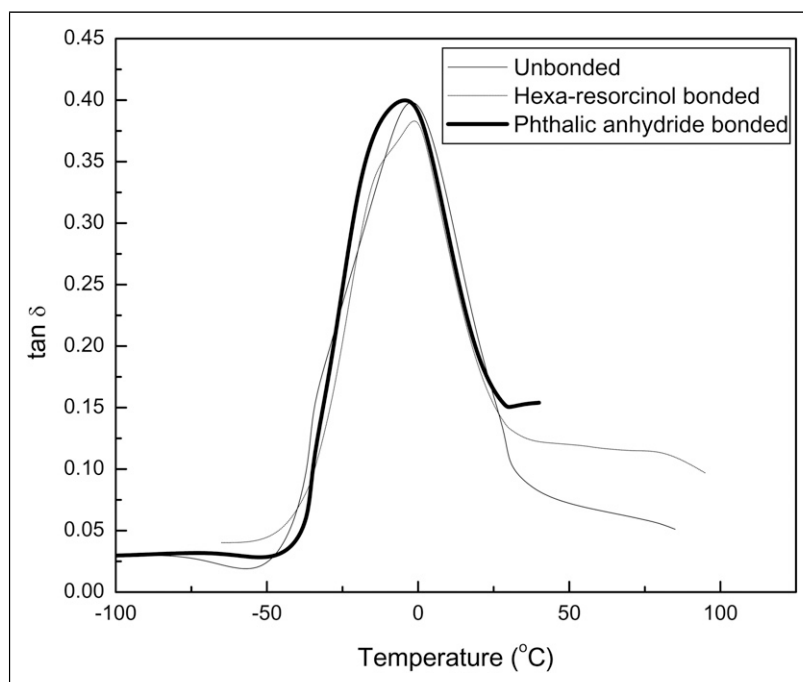


Figure 7. Variation of tan δ with temperature of unbonded and bonded composites at a frequency of 10 Hz.

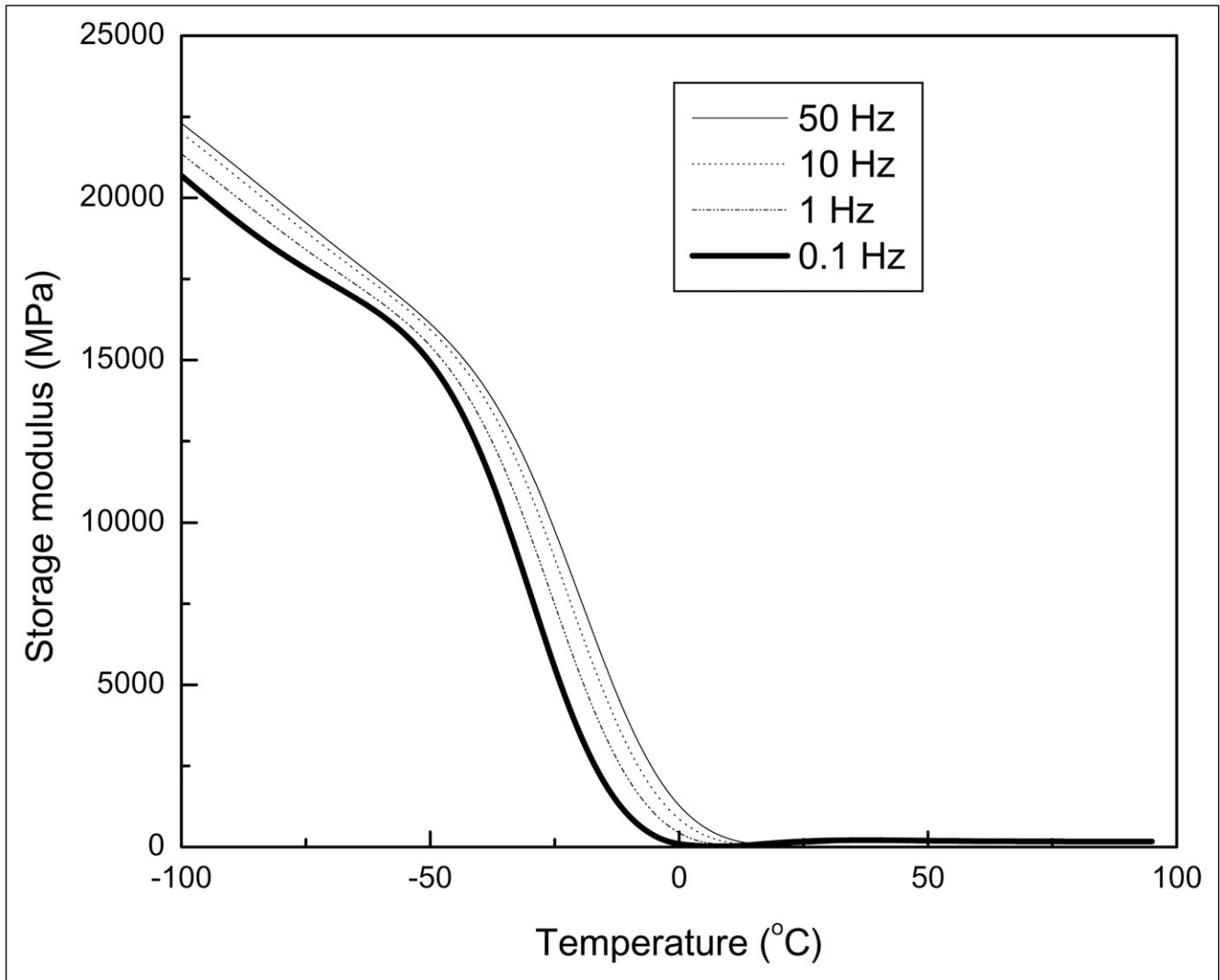


Figure 8. Effect of frequency on storage modulus ( $G'$ ) of composite containing 24 phr fibers as a function of temperature.

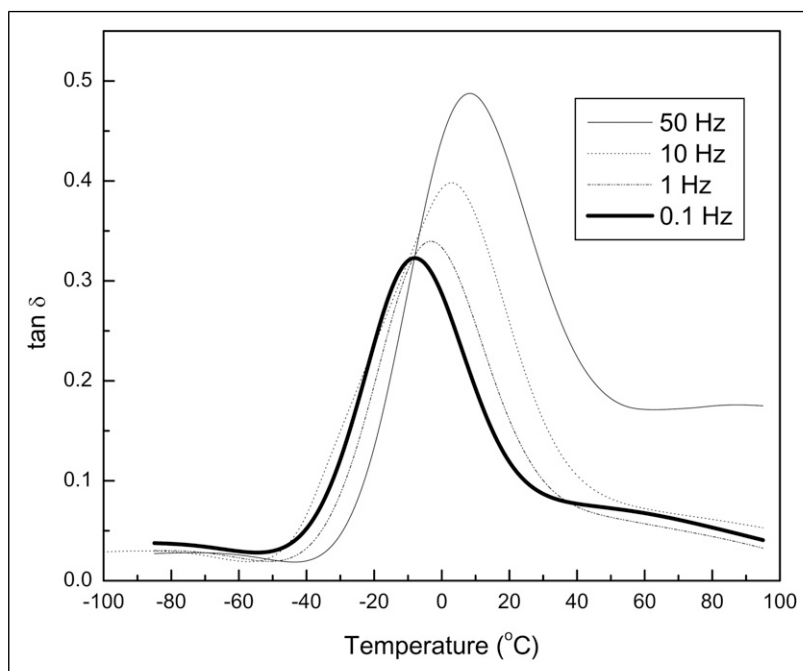


Figure 9. Effect of frequency on  $\tan \delta$  of composite containing 24 phr fibers (Mix D) as a function of temperature.

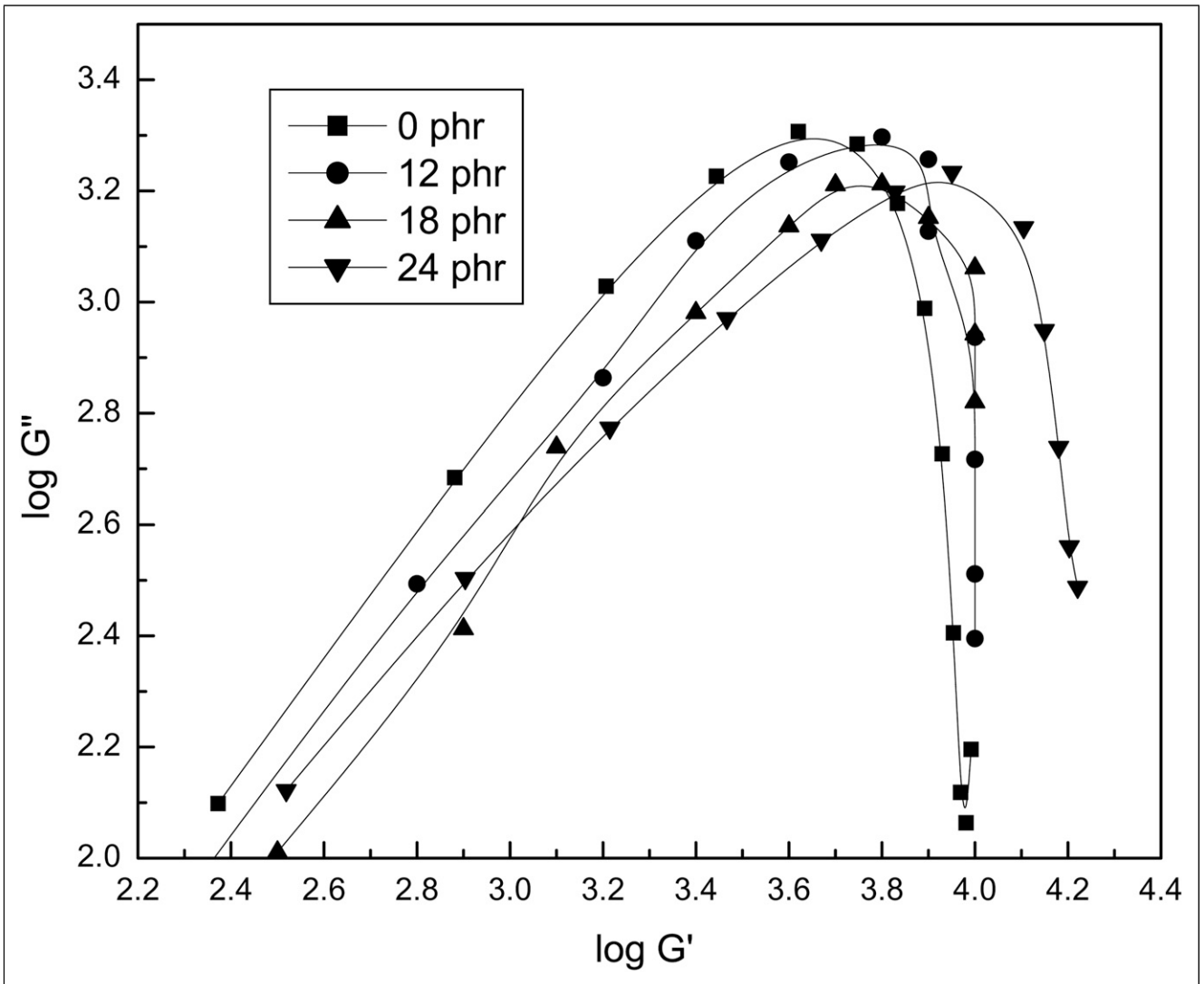


Figure 10. Cole–Cole plots of composites with different fiber loadings at a frequency of 10 Hz.

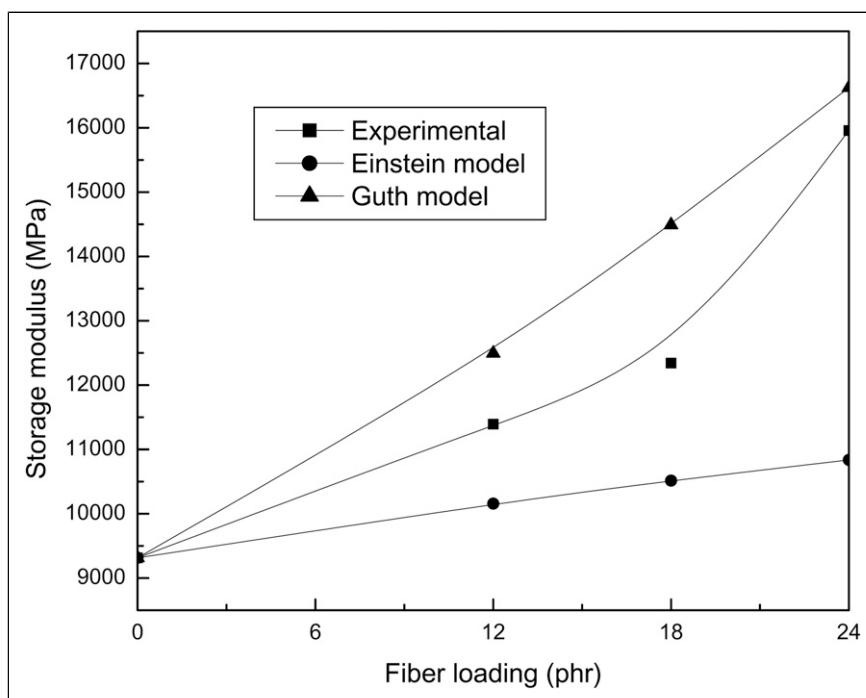


Figure 11. Comparison of experimental and theoretical storage modulus ( $G'$ ) of composites as a function of fiber loading.

## Theoretical modeling

The simplest equation for calculating the reinforcement in polymer matrix, theoretically, given by Einstein<sup>22</sup> is

$$G'c = G'm(1 + Vf) \quad (3)$$

where  $G'$  is the storage modulus, the subscripts “c” and “m” represent the composite and matrix, respectively, and  $V_f$  is the volume fraction of fiber. Einstein's equation has been modified by Guth<sup>23</sup> as

$$G'c = G'm[1 + 2.5 V_f + 14.1 V_f^2] \quad (4)$$

The experimental and theoretical storage moduli ( $G'$ ) as a function of fiber loading at a temperature of  $-50^\circ\text{C}$  and at a frequency of 10 Hz are given in Figure 11. The experimental values of the storage modulus of the composite system show a reasonably good agreement with Einstein's and Guth's models. The experimental  $G'$  values show a good agreement with Guth's model especially at 24°phr fiber loading (Mix D, Table 1). This indicates that the fiber population is just right at 24°phr loading for maximum orientation so that the fibers can actively participate in stress transfer and the composites show optimum properties.

## Conclusions

The dynamic mechanical properties such as storage modulus ( $G'$ ), loss modulus ( $G''$ ), and damping behavior ( $\tan \delta$ ) of nylon 6 fiber-reinforced NBR composites have been studied as a function of fiber loading, cross-linking systems, and bonding agents, at varying temperatures and frequencies. The storage modulus was found to be increased with increment in fiber loading, whereas it decreased with temperature. The damping characteristics were decreased with fiber loading. As the fiber loading increases, the glass transition temperature shifts to higher temperature. The DCP-cured composite showed higher storage modulus and lesser damping than the corresponding sulfur cured one. The addition of hexa-resorcinol and phthalic anhydride as bonding agents increased the storage modulus and decreased the damping. The energy of activation for glass transition of the composites was found to be increased with increase in fiber loading indicating improved interfacial adhesion. The Cole–Cole plots of the present composite systems showed the shape of imperfect semicircles pointing toward the relatively good fiber–rubber adhesion. The experimental values of the storage modulus of the composite system showed a reasonably good agreement with Einstein's and Guth's models.

## Declaration of conflicting interests

The author(s) declared no potential conflicts of interest with respect to the research, authorship, and/or publication of this article.

## Funding

The author(s) disclosed receipt of the following financial support for the research, authorship, and/or publication of this article: This study is supported by Department of Science and Technology, Govt. of India, FIST Programme (SR/FST/College-191/2014).

## ORCID iD

Rajesh C  <https://orcid.org/0000-0002-7986-3102>

## References

1. Kevin PM. *Dynamic Mechanical Analysis-A Practical Introduction*. New York: CRC Press, 1999.
2. Murayama T. *Dynamic Mechanical Analysis of Polymeric Materials*. New York: Elsevier, 1999.
3. Nielsen LE. *Mechanical Properties of Polymers and Composites*. New York: Dekker, 1974.
4. Foley ME, Abu Obaid A, Huang X, et al. Fiber/matrix interphase characterization using the dynamic interphase loading apparatus. *Composites A: Appl Sci Manufacturing* 2002; 33: 1345–1348.
5. Malas A, Pal P, Giri S, et al. Synthesis and characterizations of modified expanded graphite/emulsion styrene butadiene rubber nanocomposites: Mechanical, dynamic mechanical and morphological properties. *Composites B: Eng* 2014; 58: 267–274.
6. Flaiifel MH, Ahmad SH, Hassan A, et al. Thermal conductivity and dynamic mechanical analysis of NiZn ferrite nanoparticles filled thermoplastic natural rubber nanocomposite. *Composites Part B: Eng* 2013; 52: 334–339.
7. Durante M, Langella A, Formisano A, et al. Dynamic-mechanical behaviour of bio-composites. *Proced Eng* 2016; 167: 231–236.
8. Surajarusam B, Hajjar-Garreau S, Schrodj G, et al. Comparative study of pineapple leaf microfiber and aramid fiber reinforced natural rubbers using dynamic mechanical analysis. *Polym Test* 2020; 82: 106289.
9. Palani S, Prabhukumar S and Lakshmanan P. Dynamic mechanical analysis of areca/kenaf fiber reinforced epoxy hybrid composites fabricated in different stacking sequences. *Mater Today Proc* 2021; 39(4): 1202.
10. Surya Nagendra P, Prasad VVS and Ramji K. A study on dynamic mechanical analysis of natural nano banana particle filled polymer matrix composites. *Mater Today Proc* 2017; 4(8): 9081–9086.
11. Feiyu T, Ling C, Xinwu X, et al. Dynamical mechanical properties of wood-high density polyethylene composites filled with recycled rubber. *J Bioresour Bioprod* 2021; 6: 152–159. DOI: [10.1016/j.jobab.2021.02.007](https://doi.org/10.1016/j.jobab.2021.02.007).

12. Marcovich NE, Reboredo MM and Aranguren MI. Mechanical properties of woodflour unsaturated polyester composites. *J Appl Polym Sci* 1998; 70: 2121–2131.
13. Geethamma VG, Kalaprasad G, Groeninckx G, et al. Dynamic mechanical behavior of short coir fiber reinforced natural rubber composites. *Composites Part A: Appl Sci Manufacturing* 2005; 36(11): 1499–1506.
14. Tan JK, Kitano T and Hatakeyama T. Crystallization of carbon fibre reinforced polypropylene. *J Mater Sci* 1990; 25: 3380–3384.
15. Murayama T. *Dynamic Mechanical Analysis of Polymeric Materials*. New York: Elsevier, 1978.
16. Maurer FHJ. An interlayer model to describe the physical properties of particulate composites controlled interphases compos mater. In: *Controlled Interphases in Composite Materials*. New York: Elsevier, 1990, pp. 491–504.
17. Thoamson J L. The interface region in glass fibre-reinforced epoxy resin composites: Characterization of fibre surface coatings and the interphase. *Polym Compos* 1990; 11(2): 105.
18. Rajesh C, Unnikrishnan G, Purushothaman E, et al. Cure characteristics and mechanical properties of short nylon fiber-reinforced nitrile rubber composites. *J Appl Polym Sci* 2004; 92: 1023–1030.
19. Rajesh C, Unnikrishnan G and Purushothaman E. Investigation of interfacial adhesion in nylon-6 fibre/NBR composites through restricted equilibrium swelling technique. *Compos Inter* 2008; 15: 527–548.
20. Folkes MJ. *Short Fibre Reinforced Thermoplastics*. New York: Wiley, 1982.
21. Ibarra L. The effect of a diazide as adhesion agent on composite materials consisting of an elastomeric matrix and short polyester fiber. *J Appl Polym Sci* 1993; 49: 1595–1601.
22. Einstein A. *Investigation on Theory of Brownian Motion*. New York: Dover, 1956.
23. Guth E. Theory of filler reinforcement. *J Appl Phys* 1945; 16: 20–25.